Investigaciones Geográficas • Instituto de Geografía • UNAM
eISSN: 2448-7279 • DOI: https://doi.org/10.14350/rig.60914 • RESEARCH PAPERS
Issue 116 • April • 2025 • e60914
www.investigacionesgeograficas.unam.mx

Photogrammetry to Assess the Recovery of a Forest: Case Study of Guadalupe Island

Fotogrametría para evaluar la recuperación de un bosque: caso de estudio de Isla Guadalupe

Laura Abigail Vera-Ortega,* Alejandro Hinojosa-Corona** and Luciana Luna***

Received: 06/24/2024. Accepted: 10/22/2024. Published: 03/10/2025.

Abstract. This study employs photogrammetry to evaluate and monitor the recovery of the cypress forest on Guadalupe Island, Mexico, an ecosystem significantly impacted by fires and overgrazing. Two drone surveys were conducted over the forest area during the summers of 2016 and 2019 using natural color (RGB) and near-infrared (NIR) cameras. This work presents the first complete 3D reconstruction of the cypress forest on the island. The image processing products include the canopy height model (CHM), digital surface model (DSM), and digital terrain model (DTM), which were utilized to calculate the number, density, height and crown projected areas of trees. The CHM showed a high correlation with the forest's structure (R = 0.92), based on field measurements of tree heights. Our study accounted for approximately 67,340 trees taller than two meters in 2019. Over 90% of the cypress population consisted of young trees between 2 and 3 meters tall, which have recovered significantly following a fire in 2008 that burned 70% of its extent. A horizontal expansion of 134 hectares was observed from 2016 to 2019 in the regeneration process.

Keywords: Aerial Drone Surveys, Cypress Forest, Vegetation Structure, Canopy Height Model, Forest Regeneration.

Resumen. Este estudio emplea fotogrametría para evaluar y monitorear la recuperación del bosque de ciprés en la Isla Guadalupe, México, un ecosistema impactado por incendios y pastoreo excesivo. Se realizaron dos campañas de vuelo con drones sobre el área forestal durante los veranos de 2016 y 2019 utilizando cámaras de color natural (RGB) e infrarrojo cercano (NIR). Se presenta la primera reconstrucción completa en 3D del bosque de ciprés de la isla. Los productos de procesamiento de imágenes incluyen el modelo de altura del dosel (CHM), el modelo digital de superficie (DSM) y el modelo digital del terreno (DTM), que se utilizaron para calcular el número, la densidad, la altura y las áreas proyectadas de la copa de los árboles. El CHM mostró una alta correlación con la estructura del bosque (R = 0.92), según mediciones de campo de las alturas de los árboles. En nuestro estudio se reportan ~ 67 340 árboles de más de dos metros de altura en 2019. Más del 90% de la población de cipreses estaba formada por árboles jóvenes de entre 2 y 3 metros de altura, que se han recuperado significativamente después de un devastador incendio en 2008 que quemó el 70% de su extensión. Se observó una expansión horizontal de 134 hectáreas de 2016 a 2019.

* Departamento de Geología, Centro de Investigación Científica y de Educación Superior de Ensenada (CICESE), Carretera Ensenada-Tijuana 3918, Zona Playitas, 22860, Ensenada, Baja California, México. https://orcid.org/0000-0002-3172-0137. Email: abibaca@gmail.com.
* Departamento de Geología, Centro de Investigación Científica y de Educación Superior de Ensenada (CICESE), Carretera Ensenada-Tijuana 3918, Zona Playitas, 22860, Ensenada, Baja California, México. https://orcid.org/0000-0002-2282-337X. Email: alhinc@cicese.edu.mx. Corresponding author.
** Grupo de Ecología y Conservación de Islas (GECI), A.C. Moctezuma 836, Zona Centro, 22800, Ensenada, Baja California, México. https://orcid.org/0000-0001-7541-3334. Email: luciana.luna@islas.org.mx

Palabras clave:, levantamiento aéreo por dron, bosque de ciprés, modelos altura de dosel, estructura vertical de vegetación, regeneración del bosque.

INTRODUCTION

Remote sensing techniques enable the assessment of changes in the landscape from diverse perspectives, they are effective tools in the study of forests. Photogrammetry (aerial or satellite) is an alternative to laser scanners to model the three-dimensional (3D) structure of the surface (Nolan et al., 2015), to estimate a forest canopy height model (Cunliffe et al., 2016; Granholm et al., 2017; Lisein et al., 2013) its changes after a disturbance, or even to estimate the population range (Gallardo-Salazar & Pompa-García, 2020).

Photogrammetry is an accessible remote sensing technique based on the processing of digital images that allows the production of 3D models of objects or surfaces (Rahaman, 2021). The color of photogrammetric point clouds adds a surface texture to the analysis. Although vegetation indices (VI) can be derived from natural color (RGB) images, the high reflectivity of vegetation in the near infra-red band can be exploited from infrared images to discriminate live from dead vegetation. VI derived from infrared images will enhance the vegetation classification and filtering (Candiago et al., 2015; Moskal et al., 2000; Viljanen et al., 2018).

The vertical structure of a forest is the outcome of these persistent processes through space and time (Gadow et al., 2012; Granholm et al., 2017; Valverde & Silvertown, 1997). The forest structure is the vertical and horizontal projection of it and can be described by the canopy height and cover, leaf area density profile, and stem diameter (Brokaw, 1999; Donnellan A. et al., 2021). All these attributes allow us to assess managed and unmanaged ecosystems and analyze the heterogeneity according to disturbances and natural mechanisms of regeneration (Gadow et al., 2012).

Guadalupe Island of volcanic origin, the 7th largest island of Mexico with 243.6 km^2 is a Biosphere Reserve located in the eastern north Pacific near the Baja California coast, Mexico (Figure 1). This island is home to many endemic and native species of flora and fauna (Junak et al., 2005; Moran R., 1996; Oberbauer et al., 2009; Santos del Prado & Peters, 2005). This reserve has been affected by human activity; in the terrestrial ecosystem, the introduction of exotic invasive species caused a decrease in biodiversity, plant coverage, and loss of soil (Junak et al., 2005; Luna Mendoza et al., 2005; Oberbauer et al., 2009; Santos del Prado & Peters, 2005). The None-Governmental Organization (NGO) Grupo de Ecología y Conservación de Islas (GECI), Mexican government institutions (CONANP, CONABIO, SEMARNAT) and Mexican and international donors have worked together during the last decades making remarkable restoration and conservation efforts in this place. The eradication of feral goats was one of the most important management practices and was completed in 2007. This activity resulted in the recovery of plants (both native and non-native) in large areas (Keitt et al., 2005; Rodríguez-Malagón et al. 2007; Santos del Prado & Peters, 2005).

The island presents a climatic gradient due to its elevation (1,298 m), its north-south orientation, and the influence of dominant northwestern winds and the California Ocean current. These prevailing conditions bring humidity preferably to the northwest of the island which is captured by vegetation in the higher parts; the extrusion of the island and its attitude against predominant winds, fosters the recurrent formation of Kármán vortexes at the lee side of the island (Horváth et al., 2020). The persistent humidity allowed the establishment of forests of Guadalupe Monterey Pine (*Pinus radiata* var. *binata)*, Island Oak (*Quercus tomentella)*, and Guadalupe cypress (*Cupressus guadalupensis)* in the higher areas (Santos del Prado & Peters, 2005; Villanueva Díaz et al., 2015).

Guadalupe Island has a temperate-dry climate, characterized by wet, cold conditions in winter and warm, dry conditions in summer. The island's landscape changes seasonally: in winter, increased humidity supports the growth of annual vegetation, turning the landscape green, while in summer, a contrast emerges between dry and evergreen plants. The Guadalupe Cypress, an evergreen species, remains distinguishable during summer, with the

exception of *Calystegia macrostegia*—an evergreen shrub found in the island's northern areas. The Guadalupe Monterey pine is also evergreen but occupies different patches in the northern part of the island.

The cypress forest is the most extended tree community on the island. It is distributed in the highlands between 800 and 1200 m above sea level, forming three patches or remnants with different sizes and densities (Ramírez, 2014; Rodríguez-Malagón et al. 2007). These remnants are valuable because they provide habitat for wildlife, and contribute to local ecosystem functions such as pollination, carbon sequestration, and soil stabilization. The tree community showed an evident recovery after the goat eradication (Keitt et al., 2005), at least 7,307 mature cypress individuals were reported in 2006 (Rodríguez-Malagón et al. 2007), and the growth of hundreds of seedlings around those trees. However, in 2008, an extensive fire killed 70% of the adults and new recruits leaving a substantial extension of burned surface and few live individuals (Ramírez, 2014) (Figure 1). Despite the fire, the forest had a significant recovery due to the cones of these trees; they are serotinous and are sealed until a fire or heat opens them. Also, they had beneficial conditions for the growth of new individuals because of soil components after the fire (Oberbauer et al., 2009). Currently, the Guadalupe Island cypress forest has a significant number of individuals that grew after 2008.

Other authors have studied the Guadalupe Island cypress forest using remote sensing techniques. Rodríguez-Magalón (2007) did a multispectral analysis with a Quickbird (2004/04/24) high spatial resolution satellite image to estimate the number of trees and described the distribution of the forest patches. Ramírez (2014) calculated the cypress forest's extent using multispectral aerial and high spatial resolution satellite images from 2001 to 2012, estimating different VI to locate healthy vegetation and delineate burned areas; along with the opened and closed spaces within the forest patches. Ramírez (2014) reported three forest patches and described their extension after the 2008 fire: north, central, and south patches (Figure 1D). The north patch with an area of 9.4 hectares (ha) was completely burned, no live trees after the fire; in the central patch a similar scenario, 93% of the extent (56.3 ha) was burned; and in the south remnant (131.5 ha) 56% was burned leaving the biggest area with living trees (Figure 1).

Yépez-Rincón et al. (2021) developed a 3D Structural Classification Method using Terrestrial Laser Scanner data. This study describes the vertical structure of two sites in the cypress forest, incorporating a crown envelope descriptor mentioned as individual shape index, and with high accuracy results between field measurements and laser data. They reported a coefficient of determination R^2 = 0.949 for Diameter Breast Height, R^2 = 0.974 for the crown, and R^2 = 0.97 for heights between maximum laser pulse of tree heights and crowns in relation to field measurements.

This study aims to provide a comprehensive 3D reconstruction of the Guadalupe Island cypress forest and assess its recovery over time. Its objectives are 1) to prove that photogrammetry is a suitable and accessible technique to model the 3D structure of Guadalupe Island Cypress Forest; 2) to assess the recovery and changes of the forest after the 2008 fire using photogrammetry and multispectral analysis.

MATERIALS AND METHODS

Two field campaigns were conducted to gather aerial high spatial resolution images with Remotely Piloted Aircraft Systems (RPAS) flying over the cypress forest to map its extent and vertical structure. One survey occurred in July 2016, and the other in June 2019. Flight missions were planned with a 75% lateral and longitudinal overlap.

For the 2016 campaign, we utilized an eBee classic fixed-wing unit (FWU) equipped with two different payloads: an RGB camera and an NIR camera. The NIR camera, a modified Canon S110 unit (UAVSenseFly, 2024), captured images with three bands: NIR (850 nm), Red (625 nm), and Green (550 nm). These bands facilitated the computation of Normalized Difference Vegetation Indices (NDVI), which were used to differentiate live vegetation from dead vegetation. The FWU

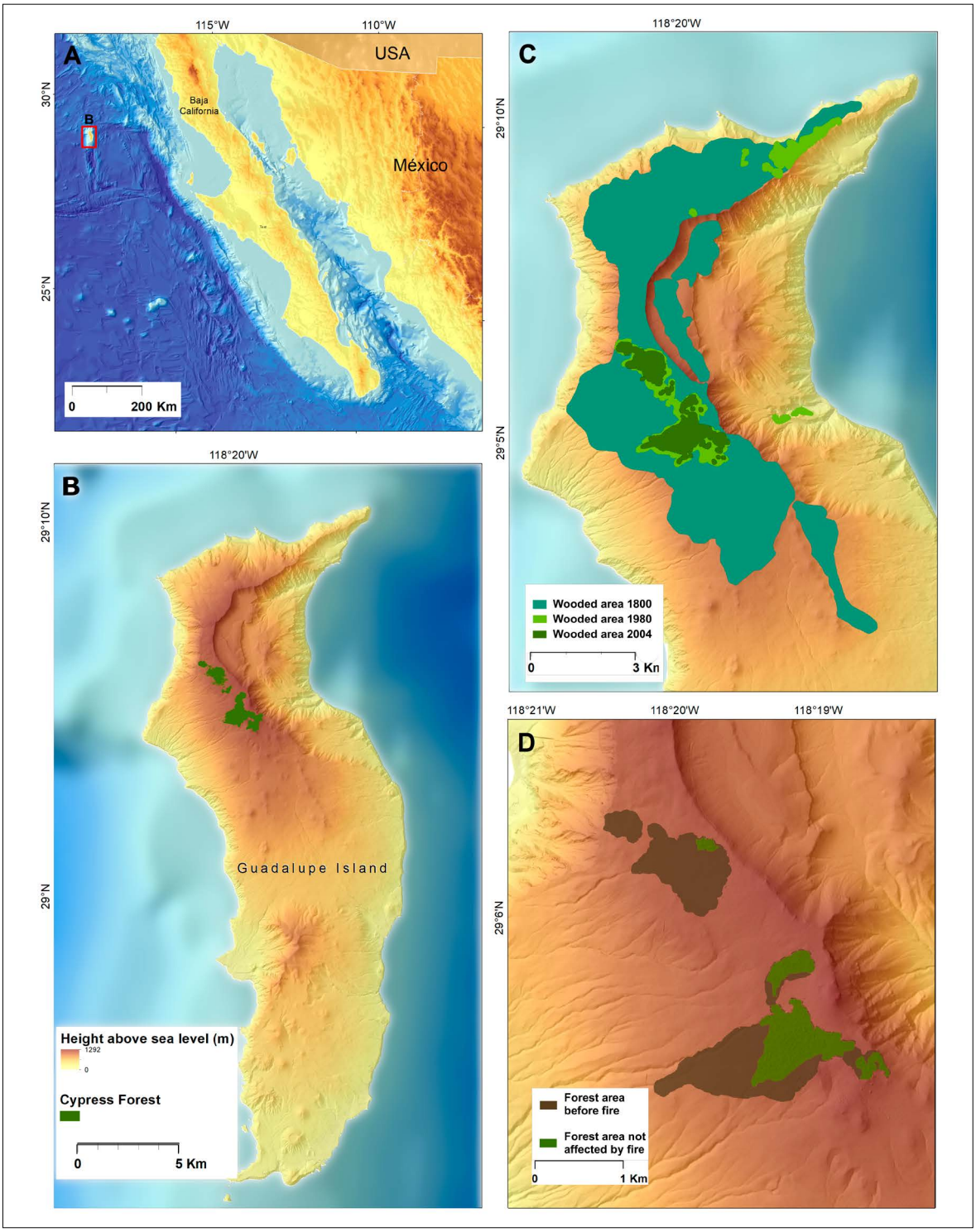

Figure 1. A) Guadalupe Island macro-location, B) Cypress forest distribution in 2019, C) Historical distribution of cypress forest from 1800 until 2004, modified from Rodríguez-Malagón (2007), D) Distribution of cypress forest in 2009, showing the area affected by the 2008 fire. Source: modified from Ramírez (2014).

RPAS allowed for extensive coverage in fewer flights, including crossed flight lines, which enhanced 3D reconstruction accuracy. It also supported terrain-aware flights, maintaining a constant altitude relative to the ground. The dual payloads of the FWU (RGB and NIR) produced two complementary datasets for the same area and timeframe (July 2016).

The eBee classic or a similar FWU was unavailable for the 2019 aerial survey. Instead, a DJI multirotor RPAS (Phantom 4 Pro) was deployed. Although effective, the multirotor system was less suited for covering large areas (1,000 ha) than the FWU. Consequently, crossed flightlines were not feasible in 2019, nor were terrain-aware flight capabilities. Only an RGB camera was employed for this campaign.

During field campaigns, Ground Control Points (GCPs) and the centers of plots were precisely geolocated with survey grade GNSS systems (Figure 2). Base and rover units were deployed, Topcon GR5 and Emlid Reach units were used in 2016 and 2019 respectively. In June 2019, 24 alea-

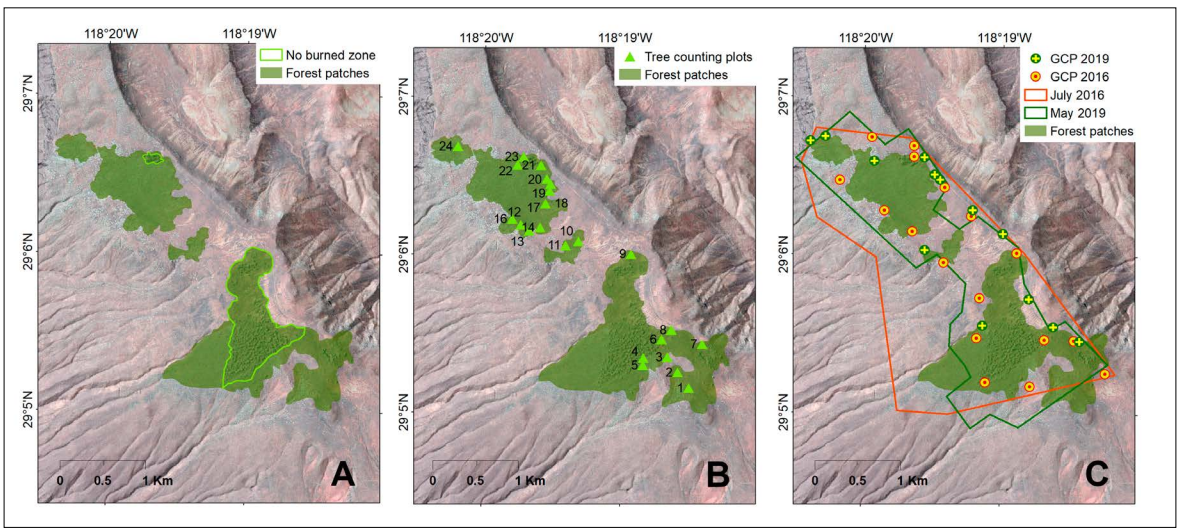

Figure 2. A) Cypress forest patches extents in 2019, showing the burned and unburned zones in central and south patches, B) Plot locations used to count and measure trees in 2019, C) Flight coverage for each survey and locations of ground control points (GCP). As backdrop a Worldview 2013 satellite image.

Table 1. Remotely Piloted Aircratf System (RPAS) flights made over the cypress forest in 2016 and 2019 (GCPs = ground control points).

Date	RPAS	Camera	Flight area	Number of flights	GCPs	Height of flight over the ground
July 2016	Fixed wing drone - eBee Classic SenseFly	SONY WX, 18 MP **RGB**	1,000 ha	11	19	130 m Terrain awareness cross lines/grid
July 2016	Fixed wing drone - eBee Classic SenseFly	CANON S110, 12 MP **NIR**	1,000 ha	10	19	130 m Terrain awareness cross lines/grid
June 2019	Multirotor DJI Phantom 4 Pro	1CMOS 20 MP **RGB**	600 ha	12	13	100 m

tory plots were traced over the forest area to count trees taller than 2 m and register their heights. Circular plots were outlined in the field with a radius of 12 m (~450 m^2 area). The reproductive status of every tree was also registered (presence of male and female cones).

In the initial growth stage, the Guadalupe Cypress has a conical crown; when they reach their maximum height, their crowns are rounded or irregular (Aljos-Farjon, 2017; Moran R., 1996; Yépez-Rincón et al., 2021). Considering this fact, we classified trees into two groups according to the crown shape: Mature trees (that survived the fire) with rounded or sub-rounded crowns and young trees (that grew after the fire) with conical crowns (Figure 3).

Photogrammetry

Aerial images were processed with Pix4D software version 3.2.23, incorporating the GCPs into the workflow for a precise geolocation of derived products: the colored point clouds, Digital Surface Models (DSMs), and orthomosaics for each year and camera model. The coordinate system selected

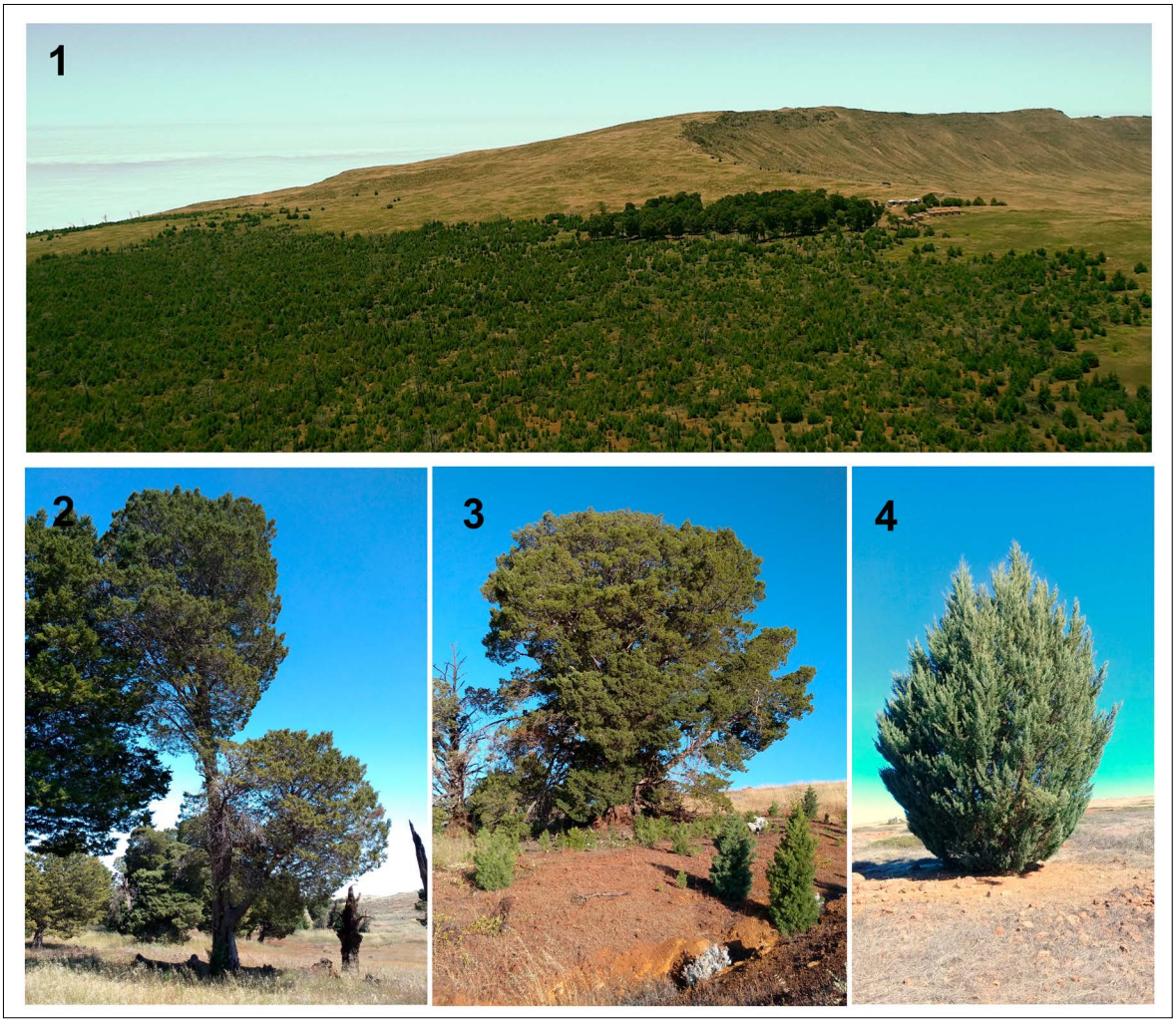

Figure 3. 1) Oblique aerial view of the central patch of the forest (facing north), where it is evident the difference between the burned and no burned area looking at the height and shape of trees. 2) Mature tree 13 m height. 3) Mature tree 12 m height, surrounded by young trees of different ages and heights. 4) A young tree of 6 m height.

for the derived products was the UTM Zone 11 North WGS84. The number of photographs and product characteristics obtained by Pix4D for each aerial survey are shown in table 2.

The Canopy Height Model (CHM) and Digital Terrain Model (DTM) were calculated from point clouds using LAStools "Efficient LiDAR Processing Software" (version 141017, academic). Custom workflows were developed to segment point clouds into tiles, to further filter, classify and calculate the CHM and DTMs. Point cloud classification is key in this process, especially identifying ground points. Once ground points are identified, the height of points from ground follow to further classify the none ground points. LAStools scripts are included as supplementary materials. The CHM is a high spatial resolution raster; it represents the canopy height of the forest over a continuous surface where the topography relief has been removed. The DTM is a high spatial resolution raster representing the ground elevation without superficial elements (trees or buildings).

An NDVI filter (>= 0.3) was applied to generate the CHM from the NIR point cloud. The result is a raster that represents only the green (live) trees. The other two RGB point clouds (2016 and 2019) were not filtered. The CHMs derived from each point cloud, are rasters with 25 cm horizontal spatial resolution (GSD) and incorporate heights between 0.1 and 24 m above ground. This GSD was chosen specifically to capture the dense growth of new trees post-2008 fire, particularly focusing on crowns and treetops of young trees that were challenging to measure in the field.

To estimate the cypress population size, 2D crown vectors, and tree top heights, we used R software version 3.6.1 (R core team 2019), using the tools from ForestTools library version 0.2.0 (Plowright, 2018). This package offers functions to analyze remotely sensed forest data derived from LiDAR or photogrammetric point clouds. We applied a workflow proposed by Plowright (2018) that uses minimum criteria on a CHM to calculate treetops and delineate tree crowns; these criteria are adjustable through a linear function, a minimum height (min-height) of treetops, and crowns. The linear function is used in the window filter algorithm to detect treetops. The linear function and min-height of trees and crowns can be established depending on the study area and features of trees that are the object of the study. In this study, we adjusted the minimum height to 2 m to account for young trees and 5 m for the mature trees. The win radius, a parameter to identify trees, was adjusted according to the patch location because of the difference in open and closed spaces (Ramírez, 2014). The burned zones (BZ) and non-burned zones (NBZ) were processed separately, with different parameters. For the NBZ in the central patch, the win radius was set to 2.5 m, while for the NBZ in the south patch was set to 3.5 m.

Table 2. Products characteristics obtained with photogrammetric process for each flight and camera for 2016 and 2019 surveys (GSD Ground Sampling Distance).

Flights	Number of photographs	Number of points in point clouds x 10^6	Density (points/m^2)	Orthomosaic GSD (cm)
RGB 2016	2346	290	30	6.5
NIR 2016	2846	316	30	6.5
RGB 2019	5219	135	20	7.5

RESULTS AND DISCUSSION

Four cypress forest patches we delimited through the NDVI analysis of a Planet dry season image (2016-08-26), contemporaneous to the 2016 aerial survey (figure 2). These patches are on the west facing slopes of the extinct volcano, near the edge of the collapsed crater. The north patch, with 11.6 hectares comprising only young trees after the fire. This patch is the most exposed to wind, with predominant rocky soil, and an average slope of 17%. The central patch with 74 hectares; it has a non-burned zone (NBZ) with mature trees and a large burned zone (BZ) with young trees. The central-south patch extends 9 hectares with only young

individuals; it is a new zone with the natural expansion of the forest, not reported by Ramírez (2014). The south patch, the largest (263 hectares) where a third of its extension was not affected by the 2008 fire, containing mostly mature trees; the remaining area is a BZ with predominantly young trees.

On the 24 plots surveyed in 2019, 638 individuals taller than 2 m were counted. Twelve of them (< 2%) were mature, and 626 were young (> 98%); the height of only 575 trees was measured because the rest were too close together, making it impossible to distinguish their individual treetops. The height range of young trees observed in the field was from 2 to 14 m: 74% less than 4 m, 18% between 5 and 7 m, and 8% between 8 and 14 m high. We registered mature trees height from 6 to 24 m. At least 68% of the counted trees had reproductive structures, in individuals from 1.5 m to 24 m.

Examples of the orthomosaics and CHMs on a BZ/NBZ transition zone are shown in Figure 4 for the two epochs and cameras in 2016. The difference between the two dates of the young trees in the BZ can be observed on the RGB orthomosaics, as well as the effect of the NDVI filter (>=3) on the 2016 NIR camera CHM, which incorporates only live trees in the model.

The comparison between CHMs of the two

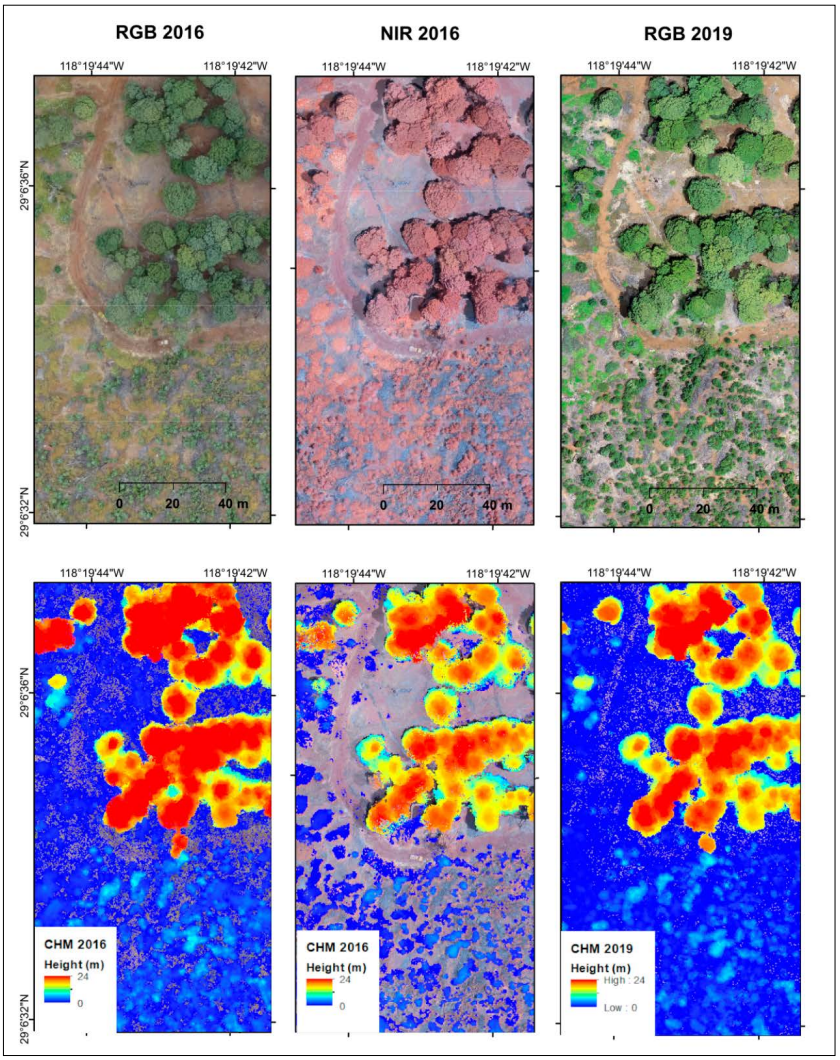

Figure 4. Mature trees in the central patch. Above are the three different orthomosaics (one per survey year/camera type); below, the corresponding CHM for each orthomosaic. A NDVI filter (>= 0.3) was applied to generate CHM from NIR images to include only green live vegetation.

dates provides information about the changes in the vertical structure of the forest, allowing us to monitor the appearance, growth and loss of trees. Examples of these results are in Figure 5.

The correlation between the number of individuals measured in the field and reported by ForestTools was R=0.65, underestimating the number of the clustered young trees and overestimating the number of mature trees. The process tended to split tree crowns of mature into more adjacent individuals. On the other end, it was not able to detect all the treetops of young trees. Despite this, it shows a positive correlation between the field measurements and ForestTools. The crown delineation closely adheres to the tree's 2D projection on the ground (Figure 7).

The correlation between tree heights measured in the field and results from ForestTools was R=0.92, showing that height values of the CHM are accurate to assess the forest vertical structure.

Table 3 shows the population of the cypress forest calculated using ForestTools, for the 2016 and 2019 surveys. The 2019 densities of individuals by patches are shown in table 4, splitting results for the burned (BZ) and non-burned zones (NBZ) in central and south patches; the areas used to calculate these densities are the areas delineated for each polygon (Figure 2). It is important to remember that the north and central-south patches have only a BZ. The NBZs are covered mainly by mature trees with heights between 6 and 21 m. However, in these areas, some young trees grew after the fire.

Table 4 shows that north and central patches have a higher density than the south and central-south patch. Also, considering the number of individuals in each patch (Table 3), we note that the central patch has the largest number of individuals, for both years and camera type. The results in height statistics are in table 5, showing the differences between BZ and NBZ.

According to table 5, the average height in

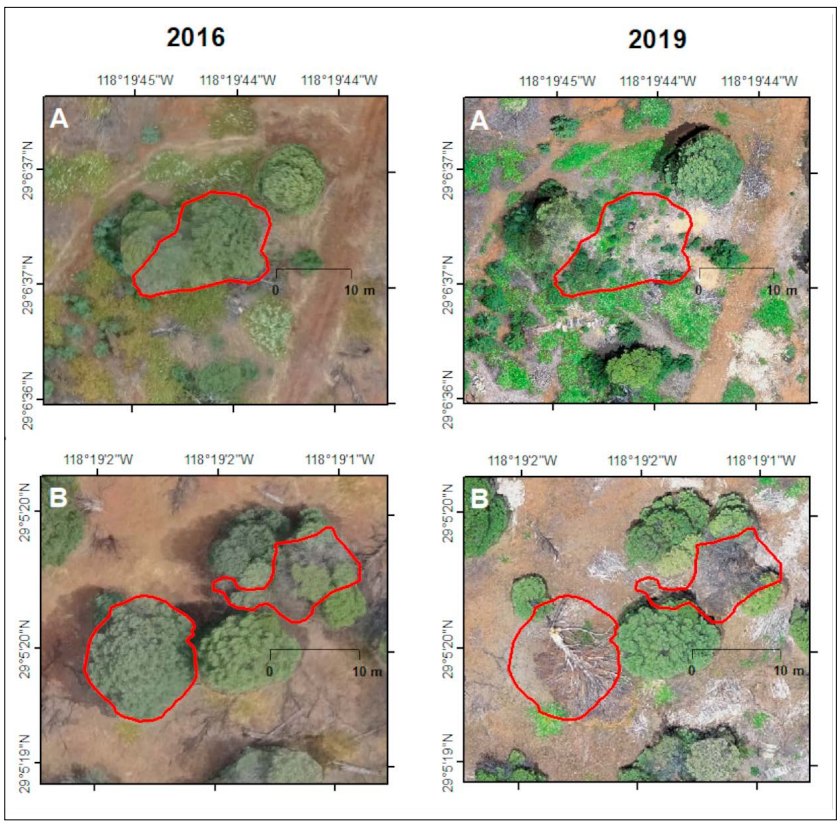

Figure 5. Example of fallen trees detected comparing CHM of 2016 and 2019.

the NBZs is greater than the average height in the BZs. The maximum value of trees in BZ of Central Patch is reported with the RGB camera, it includes standing dead trees and branches, while the maximum value in the same zone with the NIR camera represents young living trees (NDVI> 0.3).

In the south patch BZ, the maximum height reported comes from a live tree, this fact was corroborated in the field and the images. We assumed that this tree, while in the burned polygon, was not affected by fire perhaps because of the larger open spaces in this patch reported by Ramírez (2014). The average height values of all patches and zones are mostly influenced by the large number of young trees between 2 and 3 m.

Figure 6 shows the height distribution of forest patches for each survey year and camera used. Among the patches, the central patch has the highest number of trees, while the central-south patch has the lowest. Trees with heights between 2 and 3 meters are the most common across all patches, including both burned zones (BZs) and non-burned zones (NBZs). In NBZs, however, the tree population includes individuals between 11 and 24 meters, with significantly higher numbers than those observed in BZs. Additionally, the type of camera used reveals notable differences in reported tree numbers, with the 2016 RGB data showing the highest counts across all categories.

The horizontal variation of a forest can be assessed by VI using multispectral (high and medium spatial resolution) imagery. In this research, we

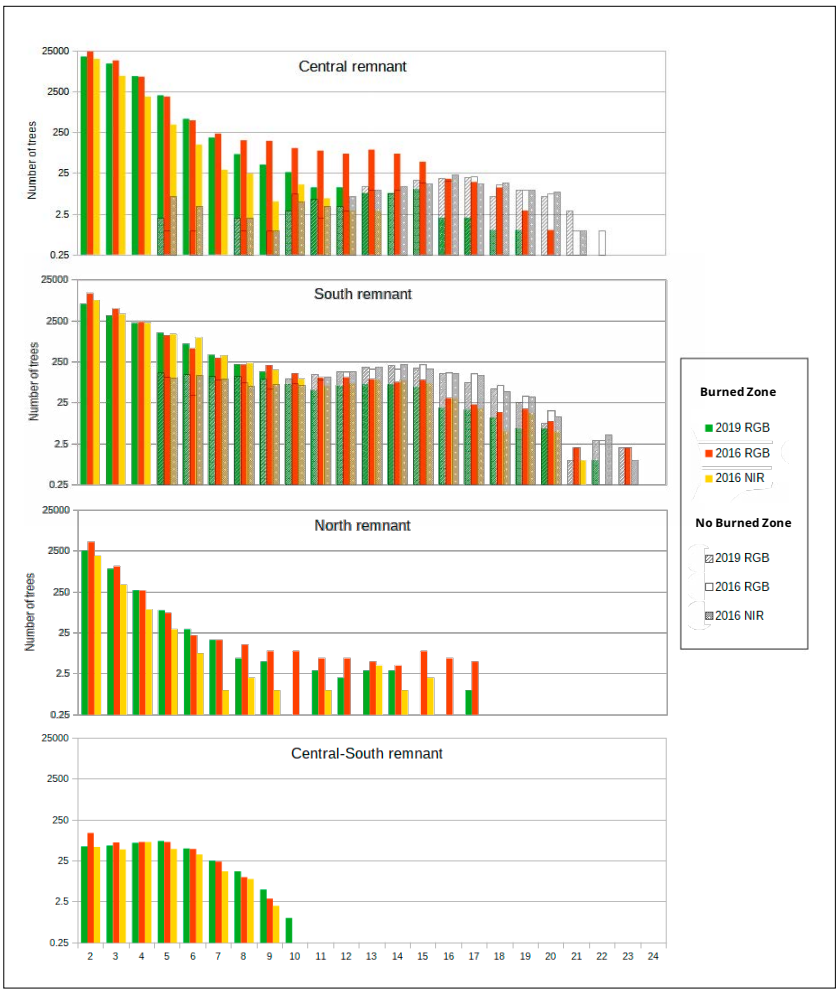

Figure 6. Tree height histograms on a logarithmic scale, in 1 m bins for the four patches analyzed during the two survey years and cameras used, breaking down the BZ and NBZ for the southern and central patches.

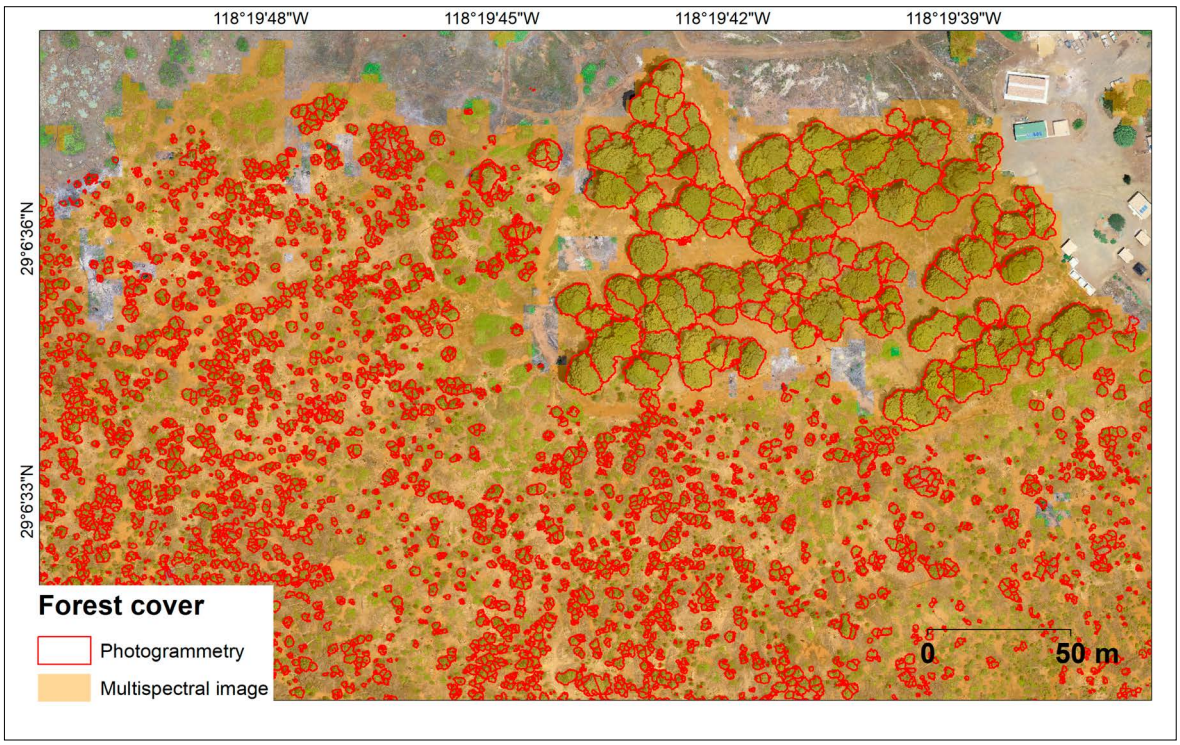

Figure 7. Comparison of vegetated areas in a portion of the central patch, where there is canopy cover from mature and young trees. Coverage delimited by NDVI > 0.3 from a planetscope multi-spectral image (August 26, 2016) compared with values delimited by ForestTools from the CHM obtained by photogrammetry using the 2016 NIR point cloud.

Table 3. The number of individuals calculated for each patch, according to the camera used and survey year.

		Number of Trees				
		Patches				
		North	Central	Central-South	South	Total
2016 NIR	Young	2 459	33 929	286	25 899	62 576
	Mature	0	120	0	1684	1,804
	Total	*2459	*34,049	*286	*27,583	*64,380
2016 RGB	Young	5 759	47 348	565	39 878	93 550
	Mature	0	122	0	1675	1 797
	Total	*5759	*48 236	*565	*41 553	*95 374
2019 RGB	Young	3 986	38 425	419	22 558	65 388
	Mature	0	138	0	1814	1952
	Total	3 986	38 563	419	24 372	67 340

*Differences between the total number of trees reported by each type of camera in 2016. There was a difference of at least 30,000 trees between the RGB and NIR in Total results. NIR results include only live trees, while RGB include live and dead-standing trees.

Table 4. Tree densities in each patch from the 2019 survey.

Patch	Trees per hectare	
	BZ	NBZ
North	344	-
Central	526	67
Central-South	40	-
South	165	24

observed the recovery and expansion of the cypress forest on Guadalupe Island after the 2008 fire, by comparing the size of the polygons reported by Ramírez (2014) and the polygons traced in this work based on 2016 Planetscope satellite images. The cypress forest showed a total increase of 134 hectares in its area, and new areas of expansion were identified like the south-central patch described in this work. This patch is a clear natural recovery zone, essential for the growth of the forest.

The tree number estimates obtained in this work from photogrammetry and Forestools correlates reasonably with field measurements (R=0.65). It underestimated the number of young trees and overestimated the number of mature trees. Gallardo-Salazar & Pompa-García (2020) used the same methodology (ForestTools algorithm) to count trees in a crop and reported a higher correlation between field measurements and ForestTools results. Ninety-five percent of the trees measured in the field were detected by the ForestTools algorithm, proving the efficiency of photogrammetry to identify and count trees. The difference in correlation results is because Gallardo-Salazar & Pompa-García (2020) analyzed a crop where the trees are regularly distributed and are the same age; unlike this study, which was performed in a forest affected by several factors and trees at different growth stages. Field observations allowed us to verify the high density of young trees in some areas of the cypress forest, where up to 30 individuals were registered in a square meter, making it difficult to measure the height of individuals in the field. The comparison of this work with Gallardo-Salazar & Pompa-García's (2020) results allowed us to determine the scope to which photogrammetry can effectively model specific ecosystems and motivated us to explore other methods.

On the other hand, this study's correlation value for height obtained using photogrammetry was high (R = 0.92). Therefore, the CHM model derived from photogrammetry proved to be an effective tool for assessing the recovery and evolution of the canopy structure and horizontal distribution of the cypress forest. It successfully generated a plausible map of tree crown geometry for the different forest patches, complemented by tree height histograms.

The difference between both surveys highlights

Table 5. Height statistics for each patch, according to the camera used and survey year. Reporting height average, maximum and standard deviation (SD). All measures in m.

		Patches					
		North	Central		Central-South	South	
			NBZ	BZ		NBZ	BZ
2016 NIR	Average	2.7	12.58	2.98	4.67	7.37	3.16
	Max	15.76	21.96	14.93	9.36	23.47	21.15
	SD	0.98	5.11	0.9	1.64	4.9	2.19
2016 RGB	Average	2.87	12.14	3.32	4.4	7.68	3.66
	Max	15.76	22.18	20.1	9.9	24	23.69
	SD	0.98	5.51	1.5	1.76	4.8	2.32
2019 RGB	Average	2.96	11.85	3.34	4.95	8.4	3.99
	Max	17.2	21.53	19.17	10.5	23	22.21
	SD	1.09	5.6	1.14	1.76	4.6	2.34

how photogrammetry results can vary depending on the study area and camera type. In the present work, the correlation was not exceptionally strong, but it was positive. Thus, the current results provide a reliable 3D description of the Guadalupe Island cypress forest, marking the first and only high spatial resolution model of this type.

Compared with vegetation studies using satellite images, photogrammetry using RPAS offers several advantages. The results of canopy cover and crown areas obtained in this work can be contrasted with those of Rodríguez-Malagón (2007), who estimated the number of individuals using high spatial resolution satellite multispectral images. Rodríguez-Malagón suggested an average canopy coverage area of 98.86 m² and 132.38 m² for mature trees. In contrast, photogrammetry results showed coverage values ranging from 2 to 104 m² for trees between 13 to 24 meters in height, with an average canopy coverage of 25 m². This demonstrates the variability and precision achievable with photogrammetric products. The full estimate of the number of individuals by Rodríguez-Malagón (2007) is not directly comparable with the present results, as the earlier study was conducted with a 2004 image pre-fire and only considered mature trees in two sizes.

Figure 7 shows the crown polygons generated by ForestTools using the photogrammetry-derived CHM, which clearly delineates the canopy projection on the ground. This method provides a more accurate approximation of the canopy cover area compared to using VI from multispectral images, where the vertical component is not included in the results.

The CHM obtained by RPAS photogrammetry accounts for the height of any type of vegetation, allowing for the discrimination of evergreen herbaceous vegetation such as *Calystegia macrostegia*.

Point clouds generated by photogrammetry have limitations in describing the vertical structure of the forest because they register only one "return" from the surface –the highest point. In contrast, laser scanners provide multiple returns from a single pulse, capturing detailed information about different layers within the vegetation. Yépez-Rincón et al. (2021) utilized point clouds from a terrestrial laser scanner to analyze tree species in specific areas of Guadalupe Island. Their study focused on cypress and pine trees, reconstructing crown geometry to differentiate between tree species effectively. This method allowed for a more detailed understanding of the vertical structure and crown architecture compared to photogrammetry.

Terrestrial and aerial LiDAR surveys are remote sensing techniques with superior capabilities for precise 3D reconstruction of the vertical structure of forests, providing detailed insights into different layers within the vegetation. However, resources to acquire LiDAR technology are not always available. Terrestrial laser scans are limited to spatial coverage due to operational limitations. Herrero-Huerta et al. (2016) successfully combined LiDAR and photogrammetry in a single aerial platform to calculate a dense CHM, but both technologies are not always available. Satellite photogrammetry offers an alternative for large-area coverage, especially with high-resolution stereo pairs or tri-stereo. Although the spatial resolution of reconstruction may not be sufficient for detailed CHM construction, potentially compromising the precision required for certain studies.

Comparing our 2016 results from NIR and RGB images, we observed a significant difference in the number of individuals counted. The NIR dataset recorded fewer trees compared to the RGB dataset. This discrepancy corresponds to the presence of standing dead trees in burned zones within patches, which were counted in the RGB dataset but ignored in the NIR dataset. Results showed the advantage of using an NIR camera and applying an NDVI filter on the resulting point cloud. With this filter, only live trees were counted offering a more precise assessment of the current living forest structure. The CHM from RGB images includes dead standing trees.

The difference between the number counted in 2016 and 2019 using RGB cameras (at least 30,000 individuals) may be due to the removal of dry material (dead-standing trees and their fallen branches), either by natural factors or human activity. Natural factors involve the removal of dry matter by wind and humidity; for example, in the northern patch, where there is no human activity, we recorded the

fall of dry trees of up to 17 m. On the other hand, human activity is evident in the south patch, where management practices are applied to prevent fires by removing fuel material. The difference between dry and live vegetation in 2016 is in Table 3, where the number of individuals counted with NIR image data (live trees) is similar to the count in 2019.

Although the loss of dead trees or large branches may explain the significant difference between 2016 and 2019, the loss of green vegetation must also be considered, especially for mature individuals. Due to their large size and weight, in addition to their shallow roots, mature individuals can be knocked down by strong winds, which are common in winter.

The number and density of trees vary between patches; the central patch accommodated the highest number of individuals and density; the north patch showed the second largest density despite its extent and substrate (mainly rock); the south patch density was at least three times lower than the central patch despite having a greater extension, and the central-south patch displayed the lowest density and number of individuals. The differences in distribution and growth of trees may be due to the environmental conditions at each patch, determined by topography and exposure to ocean moisture. The north patch is the most exposed to humidity, and thus has enough water for the trees; however, soils and exposure to winds are limiting conditions for tree growth. The central patch receives and retains the highest humidity due to its topography. Although it is exposed to winds, this patch can sustain a continuous distribution of trees. The central-south and south patches have the largest space to accommodate new trees. This also allows for the growth of the tallest individuals due to the open spaces, which was the reason why a significant number of trees in the south patch survived the 2008 fire (Ramírez, 2014).

The height distribution in each patch, in BZ or NBZ, shows the forest strata and evidences its recovery. The highest stratum is represented by mature trees, with heights between 6 and 23 m (from field observations). The most representative height frequency in this stratum is between 13 and 17 m. Table 5 shows that tree height is more variable in the areas not affected by fire (NBZs), independently of the camera used and year of survey. The NBZs contain mostly mature trees. There are two groups of young trees, those that grew immediately after the fire (2008-2009 cohort), and those that grew in the following years. The first group had heights between 4 and 12 m in 2019. The second group is represented mainly by trees between 2 and 3 m. These are trees of different generations, probably due to the seed bank that did not germinate immediately after the fire as well as the seed production of the new trees. In this work, we did not estimate the age of each stratum, but by the presence of reproductive structures in trees of 2 m height, we can assume they are a new generation. The existence of the second group of young trees is evidence of the continuous natural regeneration of the forest.

RPAS-based photogrammetry incorporates surface variability into the CHM, providing a more comprehensive representation of vegetation structure and terrain features. Additionally, the spatial resolution of photogrammetric products can be adjusted based on factors such as camera specifications and flight altitudes. This flexibility allows for the capture of high-resolution data, which is crucial for accurately assessing fine-scale variability in vegetation and terrain characteristics. Overall, RPAS-based photogrammetric analysis offers enhanced versatility and precision compared to traditional multispectral analysis, making it a valuable tool for various applications, including soil erosion modeling and ecosystem monitoring.

Study results and ancillary data may be used to validate and compared with the data from the Global Ecosystem Dynamics Investigation (GEDI) project, a high-resolution laser ranging of Earth's forests and topography from the International Space Station (ISS) (Tang et al., 2019; Wake et al., 2019). Also, with the High Resolution 1m Global Canopy Height Maps (Meta & WRI, 2023) available at Google Earth Engine and in the awesome-gee-community catalog. This dataset surged after Tolan et al. (2024), reported the first high-resolution CHMs generated by the extraction of features from a self-supervised model trained on Maxar imagery from 2017-2020. The global

dataset is contemporaneous with our results and is thus comparable to the CHMs from this study.

CONCLUSIONS

Photogrammetry, especially using drones, offers a precise and cost-effective method to model the vertical structure of the forest canopy. It allows the analysis of the temporal dynamics in a forest. The orthomosaics derived from this process have no equivalent with other satellite options due to their ultra-high spatial resolution (centimeter), sharpness, and detail, which makes them a valuable input for forest monitoring.

Our analysis provides a detailed understanding of the forest's recovery and current state, emphasizing the importance of high-resolution remote sensing in monitoring post-disturbance regeneration and forest dynamics. The reconstruction of the forest using an infrared camera (NIR) presents advantages over the use of only a natural color (RGB) camera, giving us more information on the dynamics of the forest, especially considering live and dead trees.

The estimation of the number of individuals using photogrammetry has limitations due to the conditions of natural environments that do not usually conform to ideal models. However, the CHM is representative of tree heights, as the two-dimensional grid of canopy geometry.

The Guadalupe Island cypress forest has had a significant recovery since the 2008 fire, with a total horizontal expansion of 134 hectares. Around 67,340 trees over 2 m high were counted using ForestTools, 90% are young trees between 2 and 3 m. These young individuals are distributed mainly in the areas affected by the fire and represent different generations in addition to the ones that grew immediately after the fire. The height and distribution of trees in each patch of the cypress forest are determined by biotic and abiotic conditions, being different for each patch and if they are in a burned or non-burned zone. Wind activity is an important environmental factor that affects the distribution of the trees in the cypress forest, causing the fall of live and dead trees. This phenomenon can be seen in the three years observation window (2016-2019) using photogrammetry.

AVAILABILITY OF DATA AND MATERIALS

Point clouds from the 2016 and 2019 photogrammetric reconstructions, as well as orthomosaics, digital surface models (DSMs), and canopy height models (CHMs), are available for download in https://doi.org/10.5069/G9668BDD and https://doi.org/10.5069/G92J693D. Supplemental information such as Features related to crown and treetops are accessible through CICESE's institutional repository (https://repositoriobiblioteca.cicese.mx/jspui/handle/123456789/44)

REFERENCES

Aljos-Farjon. (2017). *A handbook of the world's conifers* (second ed., vol. 1). Brill.

Brokaw, N. V. L., & L. R. A. (1999). Vertical structure. In *Maintaining biodiversity in forest ecosystems* (pp. 373-399). ML Hunter, Jr.

Candiago, S., Remondino, F., de Giglio, M., Dubbini, M., Gattelli, M., Lucieer, A., Zarco-Tejada, P. J., Rascher, U., Bareth, G., Inoue, Y., & Thenkabail, P. S. (2015). Evaluating Multispectral Images and Vegetation Indices for Precision Farming Applications from UAV Images. *Remote Sensing*, *7*, 4026-4047. https://doi.org/10.3390/rs70404026

Cunliffe, A. M., Brazier, R. E., & Anderson, K. (2016). Ultra-fine grain landscape-scale quantification of dryland vegetation structure with drone-acquired structure-from-motion photogrammetry. *Remote Sensing of Environment*, *183*, 129-143. https://doi.org/10.1016/j.rse.2016.05.019

Donnellan A., Harding D., Lundgren P., Wessels K., Gardner A., Simard M., Parrish C., Jones C., lou Y., Stoker J., Ranson K.J., Osmanoglu B., Lavalle M., Luthcke S., Saatchi S., & Treuhaft R. (2021). *Observing Earth's changing surface topography & vegetation structure: a Framework for the Decade*. NASA Surface Topography and Vegetation Incubation Study.

Gadow, K. v., Zhang, C. Y., Wehenkel, C., Pommerening, A., Corral-Rivas, J., Korol, M., Myklush, S., Hui, G. Y., Kiviste, A., & Zhao, X. H. (2012). Forest Structure and Diversity. In *Continous cover forestry* (pp. 29-83). Springer, Dordrecht. https://doi.org/10.1007/978-94-007-2202-6_2

Gallardo-Salazar, J. L., & Pompa-García, M. (2020). Detecting individual tree attributes and multispectral indices using unmanned aerial vehicles: Applications in a pine clonal orchard. *Remote Sensing*, *12*(24), 1-22. https://doi.org/10.3390/rs12244144

Granholm, A. H., Lindgren, N., Olofsson, K., Nyström, M., Allard, A., & Olsson, H. (2017). Estimating vertical canopy cover using dense image-based point cloud data in four vegetation types in southern Sweden. *International Journal of Remote Sensing*, *38*(7), 1820–1838. https://doi.org/10.1080/01431161.2017.1283074

Herrero-Huerta, M., Felipe-García, B., Belmar-Lizarán, S., Hernández-López, D., Rodríguez-González, P., & González-Aguilera, D. (2016). Dense Canopy Height Model from a low-cost photogrammetric platform and LiDAR data. *Trees - Structure and Function*, *30*(4), 1287-1301. https://doi.org/10.1007/s00468-016-1366-9

Horváth, Bresky, W., Daniels, J., Vogelzang, J., Stoffelen, A., Carr, J. L., Wu, D. L., Seethala, C., Günther, T., & Buehler, S. A. (2020). Evolution of an Atmospheric Kármán Vortex Street from High-Resolution Satellite Winds: Guadalupe Island Case Study. *Journal of Geophysical Research: Atmospheres*, *125*(4). https://doi.org/10.1029/2019JD032121

Junak, S., Keitt, B., Tershy, B., Croll, D., Luna-Mendoza, L., & Aguirre-Muñoz, A. (2005). Esfuerzos recientes de conservación y apuntes sobre el estado actual de la flora de Isla Guadalupe. In *Restauración y Conservación de la Isla Guadalupe* (pp. 83-93). Instituto Nacional de Ecología.

Keitt, B., Junak, S., Luna, L., & Aguirre, A. (2005). The Restoration of Guadalupe Island. *Fremontia*, *33*(4), 20-25.

Lisein, J., Pierrot-Deseilligny, M., Bonnet, S., & Lejeune, P. (2013). A photogrammetric workflow for the creation of a forest canopy height model from small unmanned aerial system imagery. *Forests*, *4*(4), 922-944. https://doi.org/10.3390/f4040922

Luna Mendoza, L. M., Barton, D. C., Lindquist, K. E., & Henry III, R. W. (2005). Historia de la avifauna anidante de Isla Guadalupe y las oportunidades actuales de conservación. In *Isla Guadalupe: Restauración y Conservación* (pp. 115-133). Instituto Nacional de Ecología.

Meta and World Resources Institute (WRI).(2023). High Resolution 1m Global Canopy Height Maps. https://gee-community-catalog.org/projects/meta_trees/ Accessed on 5/June/2024

Moran R. (1996). The flora of Guadalupe Island, Mexico. *Memoirs of the California Academy of Sciences*, *19*.

Moskal, L. M., Homas, S. J. T., Hall, R. J., van der Sanden, J., Franklin[2], S. E., Halll, R. J., Moskal[2], L. M., Maudie[2], A. J., & Lavigne, M. B. (2000). Incorporating texture into classification of forest species composition from airborne multispectral images. *Int. j. Remote Sensing*, *21*(1), 61-79. http://www.tandf.co.uk/journals/tf/01431161.html

Nolan, M., Larsen, C., & Sturm, M. (2015). Mapping snow depth from manned aircraft on landscape scales at centimeter resolution using structure-from-motion photogrammetry. *The Cryosphere*, *9*(4), 1445-1463. https://doi.org/10.5194/tc-9-1445-2015

Oberbauer, T., Mendoza, L. L., Oliveres, N. C., Deveze, L. B., Duarte, I. G., & Morrison, S. A. (2009). Fire on Guadalupe Island: old wounds and new opportunity. *Fremontia*, *37*(NO.3), 3-11. www.cnps.org

Plowright, A. (2018). *Canopy analysis in R using Forest Tools http://cran.nexr.com/web/packages/ForestTools/vignettes/treetopAnalysis.html*

Rahaman, H. (2021). Photogrammetry: What, How, and Where. In *Virtual Heritage: A Concise Guide* (pp. 25-37). Ubiquity Press. https://doi.org/10.5334/bck

Ramírez, N. (2014). Índices de vegetación: una herramienta para el monitoreo de esfuerzos de conservación. El caso del Bosque de Ciprés de la Isla Guadalupe. [Master thesis, Centro de Investigación Científica y de Educación Superior de Ensenada]. https://cicese.repositorioinstitucional.mx/jspui/handle/1007/1258

Rodríguez-Malagón, M. A., Hinojosa-Corona, A., Aguirre-Muñoz, A., & García-Gutiérrez, C. (2007). *The Guadalupe Island Cypress Forest: On the Recovery track*. Esri International User Conference Proceedings. Paper 1960. https://proceedings.esri.com/library/userconf/proc07/papers/papers/pap_1960.pdf

Santos del Prado, K., & Peters, E. (2005). *Isla Guadalupe: Restauración y Conservación*. Instituto Nacional de Ecología.

Tang, H., Armston, J., Hancock, S.,Marselis, Goetz, S., & Dubayah, R. (2019). Characterizing global forest canopy cover distribution using spaceborne lidar. Remote Sensing of Environment, 231, 111262. https://gedi.umd.edu/science/publications/

Tolan, J., Yang, H. I., Nosarzewski, B., Couairon, G., Vo, H. V., Brandt, J., Spore, J., Majumdar, S., Haziza, D., Vamaraju, J., Moutakanni, T., Bojanowski, P., Johns, T., White, B., Tiecke, T. & Couprie, C. (2024). Very high resolution canopy height maps from RGB imagery using self-supervised vision transformer and convolutional decoder trained on aerial lidar. *Remote Sensing of Environment*, *300*. https://doi.org/10.1016/j.rse.2023.113888

UAVSenseFly (2024). https://www.uavsensefly.cl/accesorios-camara-canon-s110-nir/. Consulted online 2024/05/15.

Valverde, T., & Silvertown, J. (1997). Canopy closure rate and forest structure. *Ecology*, *78*(5), 1555-1562.

Véga, C., & St-Onge, B. (2008). Height growth reconstruction of a boreal forest canopy over a period of 58 years using a combination of photogrammetric and lidar models. *Remote Sensing of Environment*, *112*(4), 1784–1794. https://doi.org/10.1016/J.RSE.2007.09.002

Viljanen, N., Honkavaara, E., Näsi, R., Hakala, T., Niemeläinen, O., & Kaivosoja, J. (2018). A novel machine learning method for estimating biomass of grass swards using a photogrammetric canopy height model, images and vegetation indices captured by a drone. *Agriculture (Switzerland)*, *8*(5). https://doi.org/10.3390/agriculture8050070

Villanueva Díaz, J., Cerano Paredes, J., Olivares Bañuelos, N. C., Valles Perez, M., Stahle, D. W., & Cervantes Martinez Rosalinda. (2015). Respuesta cimática del ciprés (Hesperocyparis guadalupensis) en Isla Guadalupe, Baja California, México. *Madera y Bosques*, *21*(3), 149-160.

Wake, S., Ramos-Izquierdo, L. A., Eegholm, B., Dogoda, P., Denny, Z., Hersh, M., Mulloney, M., Thomes, W. J., Ott, M. N., Jakeman, H., Poulios, D., Mule, P., de Leon, E., & Blair, J. B. (2019, September). Optical system design and integration of the Global Ecosystem Dynamics Investigation Lidar. In Infrared Remote Sensing and Instrumentation XXVII (Vol. 11128, pp. 99-111). SPIE, https://gedi.umd.edu/science/publications/

Yépez-Rincón, F. D., Luna-Mendoza, L., Ramírez-Serrato, N. L., Hinojosa-Corona, A., & Ferriño-Fierro, A. L. (2021). Assessing vertical structure of an endemic forest in succession using terrestrial laser scanning (TLS). Case study: Guadalupe Island. *Remote Sensing of Environment*, *263*, 112563. https://doi.org/10.1016/j.rse.2021.112563